American Mineralogist, Volume 87, pages 829–837, 2002

Kinetics of iron oxidation-reduction in hydrous silicic melts

FABRICE GAILLARD,* BRUNO SCAILLET, AND MICHEL PICHAVANT

ISTO, CNRS, 1 A rue de la Férollerie, 45071 Orléans, cedex 02, France

ABSTRACT

The kinetics of Fe oxidation-reduction in two hydrous rhyolitic melts, one metaluminous and the other peralkaline, have been studied at 800 °C, 2kb, for melt water contents from ~5 wt% to saturation and f_{O_2} between NNO-2 and NNO + 3 (NNO = nickel-nickel oxide redox buffer). The metaluminous melt (~1 wt% FeO_T) reached redox equilibrium after 10 hours and the peralkaline one (~3 wt% FeO_T) after 3 hours. The kinetics of Fe oxidation and reduction are similar and unaffected by the presence or absence of a hydrous fluid phase. No redox front is observable in the glass as the Fe^{3+}/Fe^{2+} ratio evolves, implying that the Fe redox kinetics in hydrous silicic melts is rate-limited neither by the diffusion of H_2 nor by the mobilities of divalent cations, as observed for anhydrous basaltic melts. We propose a two-step reaction mechanism that involves: (1) virtually instantaneous diffusion of H_2 in the sample, followed by (2) slower structural/chemical reorganizations around Fe atoms. The overall redox process involving iron and hydrogen in Fe-poor, H_2O-rich melts is thus reaction-limited and obeys a first-order logarithmic rate law. The relatively slow kinetics of oxidation/reduction explains why melt Fe^{3+}/Fe^{2+} can be readily quenched in laboratory experiments. Simulation of oxidation of magmas due to H_2 exchange with wall rocks is performed using these new kinetics laws and two D_{H_2} values extracted from the literature. We demonstrate that the metaluminous composition is not significantly modified whereas the peralkaline composition undergoes important and fast changes of Fe^{3+}/Fe^{2+} during short processes such as ascent prior to Plinian-style eruptions.

INTRODUCTION

Because Fe is the most abundant heterovalent component of terrestrial magmas, the Fe^{3+}/Fe^{2+} ratio of melts or glasses is commonly used as a measure of redox conditions or oxygen fugacity (f_{O_2}). To constrain f_{O_2} precisely from glass Fe^{3+}/Fe^{2+}, numerous experimental studies have characterized the dependence of silicate melt Fe^{3+}/Fe^{2+} on f_{O_2}, melt composition, T, and P (Sack et al. 1980; Kilinc et al. 1983; Mysen and Virgo 1989; Kress and Carmichael 1991; Moore et al. 1995; Nikolaev et al. 1996; Baker and Rutherford 1996; Gaillard et al. 2001). The Fe-redox ratio of erupted lavas is commonly regarded as a window on the redox state of the magma source region (Carmichael 1991). However, the oxidation state of Fe in natural silicate melts may also reflect the interplay of numerous complex processes such as interaction with C-O-H-S fluids (Brandon and Draper 1996), change of melt composition, crystallization, and chemical exchange with host rocks. The ability of these different processes to affect the melt Fe^{3+}/Fe^{2+} ratio depends on, among other factors, their kinetics. So, to understand and model the redox behavior of natural magmas, kinetic constraints on Fe^{2+}-Fe^{3+} reaction in silicate melts are required. These kinetic constraints must involve redox couples and cover conditions that reflect those of the Earth's interior.

Currently, experimental studies aimed at characterizing the kinetics of the Fe-redox equilibrium have been conducted at 1 atm, on H-free melts (Naney and Swanson 1984; Wendlandt 1991; Cooper et al. 1996; Cook and Cooper 2000). Under these conditions, the redox half-couples involved are O_2/O^{2-} or CO_2/CO, and Fe^{3+}/Fe^{2+}. Cooper et al. (1996) have demonstrated that Fe^{2+} oxidation is rate-limited by the mobilities of divalent cations and electron holes. The mobile cations, which include Ca, Mg, and Fe, migrate from the oxidizing front toward the glass-air interface, decreasing locally the cation/oxygen ratio, whereas a second wave composed of univalent cations (mainly Na) migrates from the reduced inner part of the sample toward the oxidizing front. As stressed by Cook and Cooper (2000), because O^{2-} ions are relatively immobile in silicate melts, the fastest reaction path acting to level out redox gradients in dry silicate melts involves cation diffusion toward the glass-air interface.

The mechanisms described above may apply to the oxidation of Fe-bearing melts at the Earth's surface where O_2 is a major component. However, in the Earth's interior, free O_2 is present in negligible amounts. Furthermore, most terrestrial magmas contain C-O-H-S volatiles phases (Stolper 1982b; Blank and Brooker 1994), which introduce additional redox half-couples (H_2/H_2O, S^{2-}/S^{6+}, CO/CO_2; Candela 1986; Baker and Rutherford 1996; Moore et al. 1995; Gaillard et al. 2001). Water is by far the most abundant volatile species in magmas (Johnson et al. 1994), so that the two main redox half-couples in hydrous silicate melts are H_2/H_2O and FeO/Fe_2O_3. In such systems, the mobilities of H_2 and H_2O (or other H-bearing species) and of electron holes are most likely to dominate the kinetics and mechanisms of Fe oxidation-reduction. H_2O mobility has been investigated mostly in low-Fe rhyolitic melts. However, the relationship between H_2O diffusion and Fe^{3+}/Fe^{2+} has not yet been elucidated (Zhang et al. 1991).

First-order constraints on H_2 diffusivity in silicate melts were

* Present address: Bayerisches Geoinstitut, Universität Bayreuth, D-95440 Bayreuth, Germany. E-mail: fabrice.gaillard@uni-bayreuth.de

0003-004X/02/0007–829$05.00

provided by Chekhmir et al. (1985). They concluded that H_2 is, by far, the fastest H-bearing diffusing species in melts (D_{H_2} ~ 2.5 log units faster than D_{H_2O}). The work of Chekhmir et al. (1985) involved H_2 diffusion in either graphite- or Mn-doped nominally anhydrous albite melts. No equivalent information is presently available for Fe-bearing melts. In this paper, we present the results of an experimental study aimed at determining the kinetics of Fe oxidation-reduction in hydrous rhyolitic melts. We demonstrate in particular that the mechanism of Fe oxidation-reduction in water-bearing melts does not result from the progression of a redox front, in strong contrast to what is observed at 1 atm in air.

Experimental and analytical methods

Starting products

The experiments were performed on two rhyolitic compositions. The first one is a synthetic glass having the composition of the matrix glass of the June 15, 1991, Mt. Pinatubo dacite (Scaillet and Evans 1999; Gaillard et al. 2001). This glass was synthesized using a standard gel method (see Pichavant 1987). The gel was melted at 1400 °C, 1 bar in air (f_{O_2} = 0.2 atm) and then quenched to a glass, which was analyzed with the electron microprobe. The glass is slightly peralkaline (Table 1). It contains 1 wt% FeO_T (total iron expressed as FeO) and has a FeO concentration (analyzed by titration) of 0.34 wt%, yielding a molar Fe_2O_3/FeO ratio of 0.97. The second sample studied is a nearly aphyric natural peralkaline obsidian from Ascension Island (Harris 1983) that contains ~3 wt% FeO_T (Table 1). To test the influence of the Fe^{3+}/Fe^{2+} ratio of the starting glass, both reduced and oxidized glasses were prepared from the Ascension obsidian. The reduced glass was obtained by reacting the powdered Ascension glass under pure H_2 at 800 °C during 6 hours (Fe_2O_3/FeO = 0.09, Table 2). For the oxidized glass, the obsidian was held at 1300 °C in air during 3 hours (Fe_2O_3/FeO = 1.54, Table 2). Glasses ground in an agate mortar to a mesh size of 20 µm were loaded in either Au or $Ag_{60}Pd_{40}$ capsules (i.d. = 2.5 mm; o.d. = 2.9 mm) together with distilled and deionized water. Most experimental charges consisted of ~80 mg of glass plus 6.5 µL of H_2O, which corresponds to water-saturated conditions at 800 °C and 2 kbar. For three charges, the amount of H_2O added was 4.5 µL, corresponding to water-undersaturated conditions. Each capsule was subsequently welded shut with a graphite arc-welder and placed inside the pressure vessel.

TABLE 1. Electron microprobe analysis of the starting glasses*

	Pinatubo matrix glass	Ascension rhyolite
SiO_2	78.44	73.57
Al_2O_3	12.59	12.32
FeO_T	1.00	3.21
MnO	0.03	0.09
MgO	0.21	0
CaO	1.33	0.32
Na_2O	3.31	5.54
K_2O	2.89	4.68
TiO_2	0.17	0.24
P_2O_5	0.02	0.03
Total†	99.91	99.5
A/CNK‡	0.95	0.80

* Compositions recalculated on an anhydrous basis.
† Original total is reported.
‡ A/CNK: $Al_2O_3/(Na_2O + K_2O + CaO)$ in moles.

Experimental apparatus

All experiments were performed in three René 41 cold-seal pressure vessels (CSPV) equipped with a modified semi-permeable H_2 Shaw-type membrane made of an $Ag_{23}Pd_{77}$ alloy (Scaillet et al. 1992; Schmidt et al. 1995). Temperature was monitored using unsheathed external type-K thermocouples. Each vessel-furnace pair was calibrated under pressure (see the method of Pichavant 1987) using internal sheathed dual type-K thermocouples calibrated against the melting points of NaCl and LiCl (Schmidt et al. 1995). Overall, the temperature is known to within ±7 °C. Total pressure (~2 kbar in all experiments) was measured by a high-pressure transducer (Asco Instrument PR 851), calibrated against a 7 kbar Heise tube gauge, and is known within ±20 bar. The H_2 membrane and line are connected to a H_2 tank allowing H_2 pressures up to 70 bar to be applied. Conversely, low f_{H_2} in the membrane and H_2 line are obtained by evacuating the line with a vacuum pump that maintains f_{H_2} at <0.1 bar. H_2 pressures were measured with a Bourdon XM801 transducer calibrated against a Protais tube gauge and are known to within ±0.1 bar.

In practice, the vessel is first loaded with a given pressure of Ar. A known H_2 fugacity is then applied to the H_2 membrane and line, and temperature is increased up to 800 °C. The duration of the heating period is about 20 mn. During that period, H_2 starts to transfer across the H_2 semi-permeable membrane toward the vessel. At equilibrium, usually attained a few minutes after thermal equilibration (see below for more information on the kinetics of H_2 transfer from membrane to capsule),

TABLE 2. Time series experiments on the Ascension composition

Starting products	Reduced	Oxidized	Reduced	Oxidized	Reduced	Oxidized	Reduced	Oxidized	Reduced	Oxidized	Reduced	Oxidized
Duration (h)	0	0	3	3	7	7	24	24	48	48	96	96
Magnetite	no	no	yes	yes	yes	yes	yes	yes	yes	yes	no	no
H_2O*	~0	0	4.68	5.00	5.62	6.05	6.85	6.81	6.67	6.85	6.37	6.41
FeO_T†	3.21	3.21	2.45	2.25	2.47	2.33	2.60	2.40	2.71	2.55	3.07	3.11
FeO‡	2.80	0.82	1.90	1.45	1.77	1.64	1.85	1.73	1.90	1.81	2.00	2.05
FeO^{liq} §	2.73	0.79	1.69	1.17	1.57	1.39	1.69	1.51	1.78	1.64	2.00	2.05
$X_{Fe_2O_3}/X_{FeO}$‖	0.09	1.54	0.22	0.46	0.29	0.34	0.27	0.30	0.26	0.28	0.27	0.26

Note: All experiments were performed at P = 2 kb, T = 800 °C, f_{H_2} =12 bar, and water saturation.
* Water in the glass determined by difference on 100% of electron microprobe analysis (EMPA).
† Total iron in the glass expressed as wt% FeO determined by EMPA.
‡ Bulk FeO (wt%) analyzed by wet chemistry.
§ FeO content of the glass (wt%) obtained from the bulk FeO content by calculating out the contribution from magnetite. Magnetite proportions are obtained by mass-balance calculations.
‖ Molar Fe^{3+}/Fe^{2+} ratio of the glass. Fe_2O_3 calculated as (FeO_T-FeO^{liq}). 1.1113

f_{H_2} in the membrane is equal to f_{H_2} in the vessel and capsule. Under these conditions, the redox state imposed on the hydrous silicate melt is known from the equilibrium:

$$H_2 + 1/2\ O_2 \leftrightarrow H_2O \quad (1)$$

where

$$1/2 \log f_{O2} = \log f_{H_2O} - \log f_{H_2} - \log K_{(1)} \quad (2)$$

Equation 2 shows that, at constant temperature and pressure, f_{O_2} is directly related to f_{H_2} if f_{H_2O} is constant. In our experiments, a steady f_{H_2} can be imposed and maintained during long durations because the Shaw membrane and H_2 line have a large volume (46 cm^3) compared with the free volume of the vessel (~8 cm^3). Therefore, the H_2 membrane acts as an H_2 buffer. Another important aspect is that our experimental setup allows f_{H_2} to be varied in situ, at constant temperature and under nearly constant P_{total} (changing f_{H_2} in the membrane slightly changes pressures), which allows either reduction or oxidation cycles to be performed.

Quenching was performed by removing the vessel from the furnace and is relatively slow (about 3–5 °C/s). Gaillard et al. (2001) have demonstrated that glasses quenched at 300 °C/s and at 0.5–1 °C/s have the same Fe-redox ratios. Therefore, no modification of the Fe^{3+}/Fe^{2+} ratio is expected at the quench rates used in this study, and the Fe-redox ratios measured in quenched glasses reflect the speciation of Fe in the melts at 800 °C and 2 kbar.

Analytical methods

Major element compositions of experimental products (glasses, magnetite, hematite, and plagioclase crystals) were obtained with a Cameca-Camebax electron microprobe at the CNRS-BRGM-UO laboratories at Orléans. For crystals, the operating analytical conditions were: 15 kV accelerating voltage, 6 nA sample current, 10 s counting time on peak, and a beam diameter of 1–2 µm. For glasses, a beam diameter of 10 to 25 µm was used to minimize the migration of alkalies (e.g., Pichavant 1987; Devine et al. 1995). Concentrations of alkalies were corrected using secondary hydrous glass standards. Water concentrations of glass were estimated using the by-difference method (Devine et al. 1995) employing, as secondary standards, a set of 4 hydrous rhyolitic glasses whose water contents (2.0–6.38 wt% H_2O) have been measured by Karl-Fischer titration.

For selected samples (numbers 1–5), the homogeneity of water concentrations ($OH+H_2O$) was checked using a Nicolet 760 Magna FTIR spectrometer on doubly polished glass wafers. Four to five spectra were collected for each analyzed glass using a beam diameter of ~100 µm. Analytical procedures are similar to those described in Gaillard et al. (2001).

A wet-chemical technique was used to determine the FeO iron content of experimental products. Glass chips totaling 50–60 mg, ground under acetone to 10–20 µm mesh size, were used for each analysis. FeO iron was determined by titration with $K_2Cr_2O_7$. The uncertainty in FeO titration, calculated through standard error propagation, ranges from 0.04 to 0.08 wt% depending on the FeO content of the sample [see Gaillard et al. (2001) for details on the reproducibility and accuracy of the technique].

Experimental strategy

In this study, both constant and variable f_{H_2} experiments were performed at 800 °C and 2 kbar total pressure.

Constant f_{H_2} experiments

Ten time-series experiments were performed with a f_{H_2} of 12 bar (~NNO-0.2) using both the oxidized and reduced Ascension glasses (Table 2). These experiments provide a test of reversibility and serve to establish the kinetics of attainment of steady-state glass Fe^{3+}/Fe^{2+} ratios (interpreted as equilibrium value) for a given f_{H_2}. In addition, four experiments were carried out on the Ascension obsidian for f_{H_2} between 50 and 1.8 bar, and five on the Pinatubo glass for f_{H_2} between 50 and 1 bar (Table 3). These experiments serve to establish the equilibrium relationship between glass Fe^{3+}/Fe^{2+} and f_{H_2} at constant T, P and f_{H_2O}. To avoid magnetite crystallization observed in the time-series experiments, these experiments were systematically started by annealing at f_{H_2} = 50 bar (~NNO-1.5, see Table 3) for 48 hours. Then, f_{H_2} was brought to the desired value and conditions were kept constant for another 24 to 48 hours (Table 3).

Variable f_{H_2} experiments (oxidation/reduction cycles)

In variable f_{H_2} experiments, either oxidation or reduction cycles were performed in situ (i.e., during a given experiment) and the Fe-redox ratio of the quenched melt was monitored as a function of time. For oxidation cycles, the experiments were started by an annealing step at f_{H_2} = 50 bar for 48 hours. Then, f_{H_2} was dropped in the membrane and H_2 line by evacuating H_2 with the vacuum pump (f_{H_2} < 0.1 bar) while the temperature was kept constant. The experiments were then maintained under these new conditions for durations ranging between 0.1 and 27.5 hours, and then quenched (Table 4). Under our experimental P-T conditions, changing f_{H_2} from 50 to <0.1 bar corresponds to a change in f_{O_2} from NNO-1.5 to ~ NNO+3. For reduction cycles (performed on the Pinatubo composition only, Table 4), after the initial annealing step at f_{H_2} = 50 bar, H_2 was evacuated and a f_{H_2} <0.1 bar was maintained for a duration known to produce a crystal-free oxidized melt on the basis of the previous results (Table 4). Then, a f_{H_2} of 50 bar was re-established within the Shaw membrane and H_2 line. Conditions were kept constant for durations of between 0.66 and 6.25 hours, and the experiments were quenched (Table 4).

It must be stressed that the charge is not affected instantaneously by the f_{O_2} change that results from varying f_{H_2} in the membrane and H_2 line. The rate of change of redox conditions inside the capsule is controlled by H_2 permeability in noble metals (both capsule and membrane) and also by the free volume of the vessel. We have calculated (see Scaillet et al. 1992) the time necessary for H_2 to equilibrate in the Au capsule following an isothermal f_{H_2} drop in the membrane such as imposed in the oxidation cycles. Results range between 4 and 7 min depending on the method of estimation of the number of moles of H_2 to be transferred. This time-scale is a much shorter than that required to attain a steady-state melt Fe-redox ratio under fixed f_{H_2} (see below). However, this time-scale is of the same order of magnitude as the minimum duration necessary to observe detectable changes in melt Fe^{3+}/Fe^{2+} ratios after a change in f_{H_2} (see below). Therefore, experiments with differ-

TABLE 3. Results of equilibrium experiments under different f_{H_2} at 800 °C, 2 kb, water saturation

f_{H_2}	log f_{O_2}	ΔNNO*	Duration (h)	FeO_T wt%†	FeO (wt%)‡	Fe_2O_3 wt%§	$X_{Fe_2O_3}/X_{FeO}$‖
				Pinatubo glass			
50	–15.36	–1.43	48	0.96	0.89	0.08	0.04
20	–14.57	–0.65	70	0.96	0.87	0.10	0.05
10.1	–13.97	–0.05	72	0.96	0.85	0.12	0.06
5.1	–13.38	0.54	78	0.94	0.80	0.16	0.07
1	–11.97	1.95	73	0.95	0.64	0.34	0.16
				Ascension glass			
50	–15.36	–1.43	45	2.97	2.30	0.74	0.11
15	–14.32	–0.39	73	2.94	2.15	0.97	0.13
8	–13.77	–0.15	75	3.04	1.86	1.31	0.19
1.8	–12.47	1.45	78	3.02	1.20	2.02	0.31

* $\Delta NNO = \log f_{O_2} - \log f_{O_2}$ of the nickel-nickel oxide buffer (NNO) at P and T.
† Total iron in the glass expressed as wt% FeO determined by EMPA.
‡ Bulk FeO (wt%) analyzed by wet chemistry.
§ Bulk Fe_2O_3: (wt%) $Fe_2O_3 = (FeO_{tot}\text{-}FeO)$. 1.1113.
‖ Molar Fe^{3+}/Fe^{2+} ratio of the glass.

TABLE 4. Results of the oxidation cycles at 800 °C and 2 kb

Run number	f_{H_2} membrane (bar)	Duration at f_{H_2}<0.1 bar (min)*	FeO_T (wt%)†	FeO (wt%)‡	Fe_2O_3 (wt%)§	H_2O total wt% ‖	Phases
			Pinatubo, Au-capsule, water saturated				
1	54.1	0	0.97	0.92	0.06	5.57 (0.04)	gl, fl
2	<0.1	20	0.95	0.90	0.06	5.61 (0.05)	gl, fl
3	<0.1	40	0.96	0.78	0.2	5.58 (0.03)	gl, fl
4	<0.1	75	0.95	0.74	0.23	5.62 (0.04)	gl, fl
5	<0.1	330	0.96	0.62	0.38	5.55 (0.05)	gl, fl
6	<0.1	1140	0.76	0.55	0.46	nd	gl,fl,pl,mag
7	<0.1	1650	0.73	0.54	0.47	nd	gl,fl,pl,mag,hm
			Pinatubo, AgPd capsules, water saturated				
8	50.5	0	0.97	0.92	0.06	6.42 (0.6)	gl,fl
9	<0.1	20	0.96	0.87	0.10	6.81 (0.45)	gl,fl
10	<0.1	40	0.94	0.78	0.19	6.55 (0.44)	gl,fl
11	<0.1	75	0.95	0.75	0.24	6.79 (0.65)	gl,fl
			Pinatubo, water-undersaturated				
12	51.3	0	0.97	0.92	0.06	4.50 (0.1)	gl
13	<0.1	20	0.96	0.88	0.09	4.85 (0.1)	gl
14	<0.1	40	0.98	0.80	0.20	4.6 (0.07)	gl
15	<0.1	75	0.95	0.76	0.22	4.9 (0.1)	gl
			Ascension, Au-capsule, water saturated				
16	<0.1	0	2.97	2.30	0.74	nd	gl, fl
17	<0.1	6	3.00	2.13	0.96	nd	gl, fl
18	<0.1	40	3.04	1.98	1.32	nd	gl, fl
19	<0.1	75	3.05	1.5	1.72	nd	gl, fl
20	<0.1	150	3.04	1.26	1.98	nd	gl, fl, mag
21	<0.1	480	3.01	1.20	2.01	nd	gl, fl, mag
22	<0.1	1000	3.05	1.22	2.03	nd	gl, fl, mag

Note: gl = glass; mag = magnetite; hm = hematite; fl = vapor; pl = plagioclase.
* Before imposing $f_{H_2} < 0.1$, all samples were first annealed under 50 bar of f_{H_2} for 48 hours.
† Total Fe in the glass expressed as wt% FeO determined by EMPA.
‡ Bulk FeO (wt%) analyzed by wet chemistry.
§ Bulk Fe_2O_3: (wt%) $Fe_2O_3 = (FeO_{tot}\text{-}FeO)$. 1.1113.
‖ Total water measured by FTIR (H_2O + OH). Values in brackets correspond to maximum differences of total H_2O. For all samples 1.27<OH<1.3 wt%.

ent capsule materials have been performed to test the effect of the rate of H_2 transfer.

RESULTS

Constant f_{H_2} (equilibrium) experiments

Results for the time-series experiments are detailed in Table 2. Magnetite is present in all experiments with durations of <48 hours, irrespective of the redox state of the starting glass (either oxidized or reduced). In the two longest experiments from this series (96 hours), magnetite is not found. This magnetite thus nucleates and grows during heating-up but is not stable at the final P-T-f_{H_2}-f_{H_2O} conditions. The FeO content of the glass is obtained from the bulk FeO content of the charge (analyzed by titration) by subtracting the contribution of magnetite whose composition is known from electron microprobe analysis and whose proportion in run products is calculated by mass balance (Table 2). Results show that Fe-redox equilibrium is closely approached in the melt after experimental durations of ~10 hours (Fig. 1). A steady-state glass Fe^{3+}/Fe^{2+} ratio is attained after ~20 hours. The equilibrium glass Fe^{3+}/Fe^{2+} is approached from both sides (i.e., oxidized and reduced) and at similar rates.

Results of the equilibrium experiments are presented as a function of f_{H_2} and f_{O_2} in Table 3. All data concern crystal-free

glasses. No Fe loss from sample to capsule was detected (see total FeO contents in Table 3). Glasses have homogeneous major element compositions and water contents. Observation of the samples under an optical microscope shows that the color of the glasses is systematically related to its Fe-redox ratio. For the Ascension composition, glasses synthesized at f_{O_2} < NNO are green-blue and progressively change their color to brown-black for f_{O_2} > NNO. For the Pinatubo composition, glasses synthesized at f_{O_2} < NNO are transparent and progressively change their color to black for f_{O_2} > NNO. Analyses of different chips of the same homogeneously colored glasses (synthesized from both the Ascension and Pinatubo compositions) were performed by Gaillard et al. (2001). They yielded identical FeO contents, demonstrating that color homogeneity implies constant glass Fe^{3+}/Fe^{2+} ratio. For all samples of this study, the homogeneity of the Fe-redox state is therefore inferred from the lack of color variation across the sample. Note that experimental durations at the equilibrium f_{H_2} (i.e., following the annealing step at f_{H_2} = 50 bar) range between 22 and 30 hours (Table 3), and are therefore longer than durations necessary for attainment of steady-state Fe^{3+}/Fe^{2+} ratios (Fig. 1).

Glass Fe_2O_3/FeO values are plotted vs. f_{O_2} and f_{H_2} in Figure 2. For both starting samples, glass Fe_2O_3/FeO progressively decreases with increasing f_{H_2} (or decreasing f_{O_2}). For a given f_{H_2}, glass Fe_2O_3/FeO differ between the two compositions studied. The experimental data from this study are compared with the empirical equation of Kress and Carmichael (1991) in Figure 2a. As observed in previous studies (Baker and Rutherford 1996; Gaillard et al. 2001), there are significant differences between the measured and calculated glass Fe_2O_3/FeO, particularly for the Ascension composition in the present case.

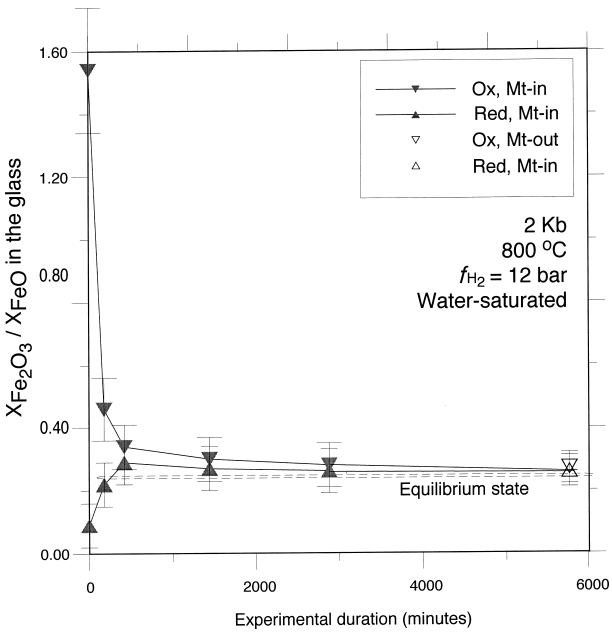

FIGURE 1. Change in glass $X_{Fe_2O_3}/X_{FeO}$ with experimental duration for time-series experiments performed on the Ascension starting composition. Data are listed in Table 2.

Variable f_{H_2} experiments (oxidation-reduction cycles)

Results of these experiments are detailed in Tables 4–5. Charges are generally crystal-free, except for the long-duration oxidation experiments (Table 4). As in the previous series, glasses are chemically homogeneous (major-element compositions and water contents, Table 4). One critical point to be stressed is the absence of any color gradient in the glasses. This feature was checked carefully through observation of doubly polished glass wafers across the entire sample section. This homogeneity is true even for glasses that have Fe_2O_3/FeO different from equilibrium values (the case for most glasses from

TABLE 5. Results of a reduction cycle at 800 °C and 2 kb performed on the Pinatubo composition

Run number	f_{H_2} membrane (in bar)	Duration at f_{H_2} ~ 55 bar (min) *	FeO_T (wt%)†	FeO (wt%)‡	Fe_2O_3 (wt%)§	Phases
23	<0.1	0	0.96	0.62	0.38	gl, fl
24	53.1	40	0.96	0.72	0.27	gl, fl
25	51.9	75	0.97	0.79	0.20	gl, fl
26	51.3	375	0.97	0.89	0.09	gl, fl

Note: gl = glass; fl = vapor.
* All samples, after being annealed under 50 bar f_{H_2}, were initially kept under f_{H_2}<0.1 for 330 min.
† Total iron in the glass expressed as wt% FeO determined by EMPA.
‡ Bulk FeO (wt%) analyzed by wet chemistry.
§ Bulk Fe_2O_3: (wt%) Fe_2O_3 = (FeO_{tot}-FeO). 1.1113.

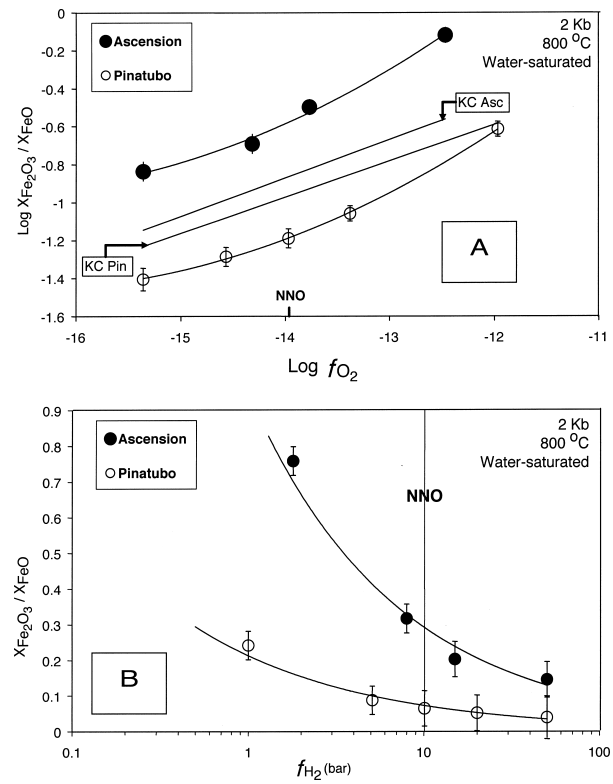

FIGURE 2. Equilibrium relationships between log $X_{Fe_2O_3}/X_{FeO}$ and log f_{O_2} (A) and $X_{Fe_2O_3}/X_{FeO}$ and f_{H_2} (B) for the two compositions studied. In A, the two lines "KCAsc" and "KCPin" represent the $X_{Fe_2O_3}/X_{FeO}$ values calculated from Kress and Carmichael (1991) for the Ascension and Pinatubo compositions, respectively. The curves fitting the experimental data are empirical formulations.

the oxidation-reduction cycles). The lack of color variation in these glasses suggests that they have uniform, though non-equilibrated, Fe_2O_3/FeO ratios.

Because Fe loss to the capsule was not detected, the evolution of the Fe-redox state upon either oxidation or reduction cycles can be represented by the change of the glass FeO concentration with time (Figs. 3–5). For an oxidation cycle (Fig. 3), glasses from both starting compositions have FeO concentrations that decrease progressively with experimental duration at f_{H_2} <0.1bar (Table 4). For the Pinatubo composition, no significant modification of the FeO concentration was detected in a glass quenched 20 min after imposing the new f_{H_2} (< 0.1 bar) in the membrane. In contrast, for the Ascension composition, a drop in FeO concentration was detected in the glass only 6 min after the imposition of the new f_{H_2} value. For both compositions, steady-state bulk FeO concentrations (0.54 wt% for Pinatubo and 1.20–1.26 wt% for Ascension) were attained after ~10 and ~3 hours respectively at <0.1 bar f_{H_2}. The results consistently show that the Ascension composition reacts more rapidly to f_{H_2} changes and suggest a dependence of the kinetics of Fe oxidation on melt composition. Partial crystallization due to high Fe_2O_3/FeO ratio of the charge is observed for the two longest experiments in both series (Table 4). For the Pinatubo composition, magnetite appears together with plagioclase, being joined by hematite in the longest experiment (Table 4). Coexisting Fe-Ti oxide compositions yield a f_{O_2} slightly higher than the MNO buffer (NNO+2.8, corresponding to $f_{H_2} \sim 10^{-3}$/bar), as calculated using the empirical calibration of Scaillet and Evans (1999). For the Ascension composition, only magnetite was observed to crystallize.

The effect of excess H_2O on the kinetics of Fe oxidation was tested by comparing the kinetic response of water-saturated ($H_2O = 6.3 \pm 0.8$ wt%) and slightly water-undersaturated ($H_2O \sim 4.7 \pm 0.6$ wt%) charges (Table 4). The rates of change of glass FeO concentrations following a f_{H_2} drop <0.1 bar, as seen on Figure 4, are identical within analytical uncertainty for water-saturated and water-undersaturated melts (both for the Pinatubo composition), suggesting that they have identical kinetics of Fe oxidation. Similarly, using $Ag_{40}Pd_{60}$ capsules instead of Au results in no difference in the rate of change of

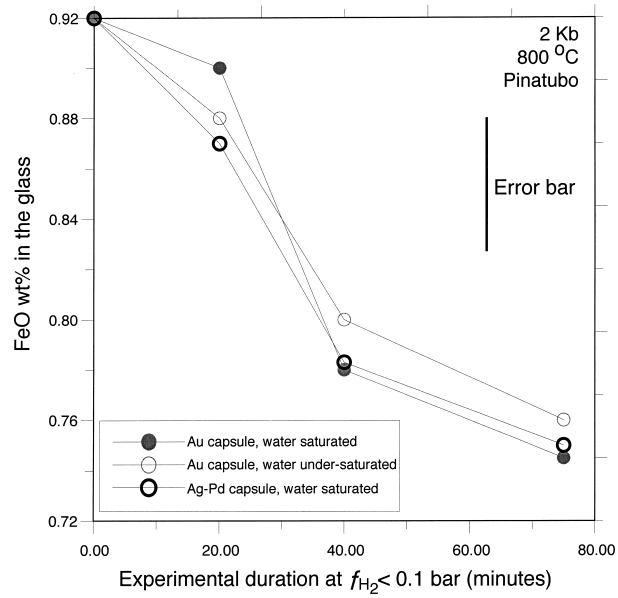

FIGURE 4. Influence of the H_2O concentration and the capsule material on the kinetics of decrease of glass FeO concentration in oxidation cycles performed on the Pinatubo composition. Data are in Tables 4.

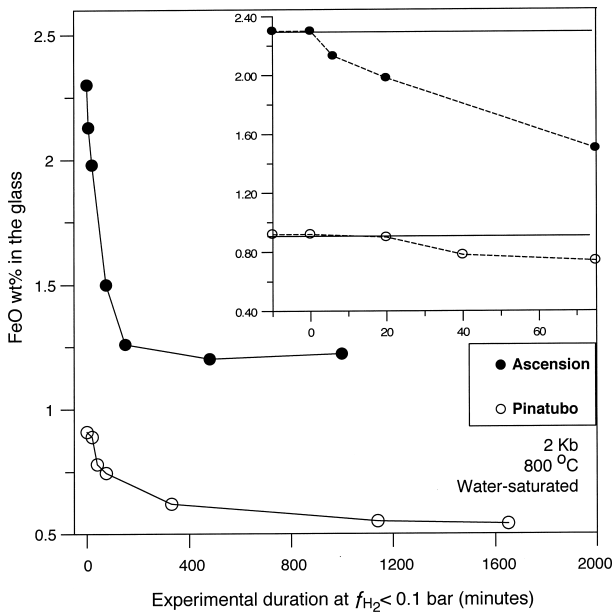

FIGURE 3. Changes in glass FeO concentrations with experimental duration in oxidation cycles performed on the Ascension and Pinatubo compositions. The inset details results for the shortest durations. Data are in Table 4.

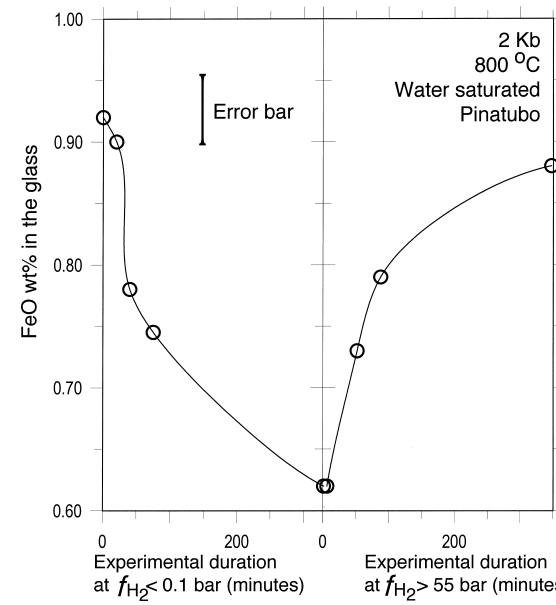

FIGURE 5. Change in glass FeO concentration with experimental duration in oxidation and reduction cycles performed on the Pinatubo composition. Data are in Tables 4 and 5.

glass FeO concentrations (Table 4; Fig. 4), despite H_2 permeability being two orders of magnitude faster in $Ag_{40}Pd_{60}$ than in Au under our experimental conditions (Chou 1986). Therefore, the kinetics of Fe oxidation is not influenced by the kinetics of H_2 transfer through the capsules.

Results of a reduction cycle performed on the Pinatubo composition are shown in Figure 5. Samples (after being annealed under 50 bar f_{H_2}) were kept under <0.1 bar f_{H_2} for 330 min. At this point, the FeO concentration of the glass was 0.62 wt% (Tables 4 and 6). Following the re-establishment of an f_{H_2} of ~50 bar in the membrane, glass FeO concentrations progressively increased with time. The highest FeO concentration (0.89 wt%), attained after 375 min at ~50 bar f_{H_2} (Table 6), is within the measured range of equilibrium FeO concentrations for 50 bar f_{H_2} (0.89–0.92 wt% FeO, Tables 3 and 5). As for the oxidation cycles, the kinetic response is characterized by an initially rapid variation of the FeO concentration of the glass, followed by a slower variation as equilibrium is approached progressively. Patterns shown by oxidation and reduction cycles are symmetrical. No difference exists between the kinetics of oxidation and reduction of Fe and the process is fully reversible (Figs. 5 and 6, see also Fig. 1).

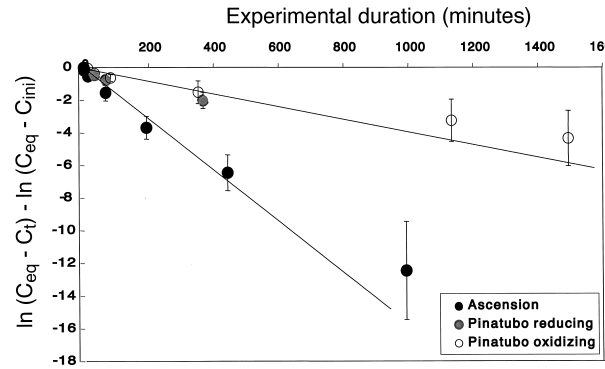

FIGURE 6. Determination of the kinetic constants for Ascension and Pinatubo compositions for T = 800 °C, 2 kb and water-saturated conditions. The fitting procedure was achieved by minimizing the differences between each calculated (from Eq. 3, see text) and measured value weighted by each experimental erro

DISCUSSION

Among the results presented above, the strong compositional dependence of the rate of change of the Fe^{3+}/Fe^{2+} ratio, together with the lack of influence of the capsule material, suggest that the main factor controlling the Fe-redox kinetics is the nature of the silicate liquids (and not the kinetics of the experimental set-up used to vary the f_{H_2} at P and T). Our results thus demonstrate that at constant f_{H_2O}, varying f_{H_2} at equilibrium with a H_2O-, Fe-bearing silicate melt leads to changes in the redox state of iron. At 800 °C, the time needed to establish a new equilibrium melt Fe^{3+}/Fe^{2+} ratio after imposition of a new f_{H_2} is on the order of several to ten hours, which is evidence for the relatively slow kinetics of the Fe-redox reaction in rhyolitic melts. This result is consistent with previous experimental findings by Gaillard et al. (2001), who demonstrated that the Fe-redox ratio of hydrous silicic melts is unchanged when varying the quench rate between 300 and 0.5–1 °C/s, suggesting that the Fe^{2+}/Fe^{3+} ratio of such synthetic and natural melts are readily quenchable.

Comparison between H-free and hydrous melts

From a kinetic point of view, it is interesting to compare the oxidation-reduction kinetics observed in this study with previous results for dry melts. The kinetics of Fe-oxidation in dry rhyolitic melts (SiO_2 = 73.4 wt%, FeO tot = 1 wt%) was studied by Naney and Swanson (1984) at T = 1343 °C in air. They found that approximately 40 hours were needed to reach Fe^{3+}/Fe^{2+} equilibrium for sample volumes similar to ours. In contrast, for compositionally equivalent but H_2O-bearing melts at 800 °C, the present study shows that equilibrium is attained in only 3–10 hours (Figs. 1 and 3). Yet, the melt viscosities in both studies are similar despite the large temperature difference: the rhyolite melt investigated by Naney and Swanson (1984) has a viscosity of 1.7×10^4 Pa·s at 1343 °C, very close to that of the Pinatubo rhyolite under our experimental T-H_2O conditions (4.38×10^4 Pa·s, calculated from Hess et al. 1996). Therefore, the melts in both studies have similar relaxation timescales (Dingwell and Webb 1990) even though the kinetics of attainment of Fe-redox equilibrium differ from each other (40 vs. 3–10 hours).

In terms of reaction mechanisms, there is a major difference between our results and previous observations made on oxidation of dry Fe-bearing melts (Cooper et al. 1996; Cook and Cooper 2000). The hydrous glass samples from this study bear evidence neither for a redox front that progresses from the capsule-sample interface toward the core of the sample, nor for cation migration, as observed in the dry systems. Another difference to be noted concerns the delay of several minutes between the application of a new f_{H_2} and the response in terms of the glass Fe^{3+}/Fe^{2+} ratio, which is most clearly seen for the Pinatubo composition (Table 4). Therefore, mechanisms of oxidation-reduction in H-bearing melts appear to differ from those identified by Cooper and co-workers in H-free melts.

Mechanisms of Fe oxidation-reduction in hydrous silicic melts

The absence of a redox front and redox heterogeneity in the glasses, despite gradual changes of Fe_2O_3/FeO, is the major observation of this study. This finding suggests that the redox potentials within each part of the melt are equal but out of equilibrium. Consquently the redox process appears to be reaction-limited rather than diffusion-limited. Molecular H_2 can be transported across the sample either as a dissolved melt species (see Schmidt et al. 1998) or as a fluid species (quenched melts contain bubbles of trapped aqueous fluids). Given the high diffusion rates of H_2 in melts (Chekhmir et al. 1985), communication of f_{H_2} is nearly instantaneous at the sample scale. Partial equilibrium of the chemical potential of H_2 (μ_{H_2}) should thus be attained virtually instantaneously within the whole sample. In contrast, the delay and rate of Fe_2O_3/FeO changes after application of a new f_{H_2} indicates that $Fe^{3+} \leftrightarrow Fe^{2+}$ transformations are much slower and thus rate-limit the overall redox processes.

The microscopic phenomena driving the $Fe^{3+} \leftrightarrow Fe^{2+}$ trans-

formations are not accessible through our results. However, we note that structural (compositional) controls apply because, for the two compositions studied, two different rates of $Fe^{3+} \leftrightarrow Fe^{2+}$ transformations due to f_{H_2} changes have been measured. This difference can be attributed either to the peralkaline nature (i.e., lower viscosity) of, or to a higher Fe concentration in, the Ascension glass compared to the Pinatubo composition.

Mechanisms of interactions between H_2 and Fe-bearing silicate minerals such as pyroxene, olivine, and garnet show that hydrogenation-dehydrogenation and Fe^{3+}-Fe^{2+}reactions are coupled (Hercule and Ingrin 1999; see Ingrin and Skogby 2000, for a review). The kinetics of these reactions have been proposed to be rate-limited either by the mobility of the hydrogen atoms (at high Fe concentrations) or by the mobility of electron holes (i.e., jumps between Fe^{2+} and Fe^{3+}, at low Fe concentrations).

In this study, we have observed that the most Fe-rich melt (Ascension) has the fastest kinetics of Fe-redox equilibration, which could be consistent with the kinetic model proposed for silicate minerals. However, the analogy with minerals cannot be pursued any further because, in contrast to what was observed in NAM, there is evidence neither for mass transfer by diffusion of hydrogen-bearing species as illustrated by the homogeneous H_2O concentrations (Table 4), nor for apparent redox heterogeneity in experimental products as would be expected in the case of migration of electron holes.

Kinetics of Fe oxidation-reduction in hydrous silicic melts

Kinetic constants were extracted from the data obtained on each studied composition. For the Ascension composition, results from the oxidation cycles were used whereas for the Pinatubo composition, data from both the oxidation and reduction cycles were used. The best and simplest fit of the experimental data was obtained by considering a first-order (logarithmic) rate law (Lasaga 1998):

$$\ln(C_{eq}\text{-}C_t)\text{-}\ln(C_{eq}\text{-}C_{in}) = k.t \quad (3)$$

where C_{eq} is the equilibrium Fe^{3+}/Fe^{2+} concentration, C_{in} the initial Fe^{3+}/Fe^{2+} concentration, C_t the Fe^{3+}/Fe^{2+} concentration at time t, and k the first-order rate constant. The fitting procedure is explained in the caption of Figure 6. The extracted values yield k = 0.003/min for the Pinatubo and k = 0.0152/min for the Ascension composition (Fig. 6). The fact that the data obey first-order logarithmic kinetics confirms that the overall process is rate-limited by the $Fe^{3+} \leftrightarrow Fe^{2+}$ transformations, and not by the diffusion of H_2, which can be considered instantaneous.

Geological application

This study shows that f_{O_2} changes can be driven by f_{H_2} changes. Hereafter, we model changes in melt Fe^{3+}/Fe^{2+} that result from H_2 exchanges between a silicic magma (assumed to have the composition of the Pinatubo and Ascension samples) and its host rocks. The principle of the simulation is to impose an initial f_{H_2} difference between the two reservoirs (melt and host rocks), and to calculate, for a given duration, the gradient in f_{H_2} and the associated change in Fe^{3+}/Fe^{2+} that results from diffusive exchange of H_2. Only lateral transfer of H_2 is considered (Figs. 7A and 7B). The simulations may best apply to magma ascent into a conduit during a volcanic eruption. The starting f_{H_2} of the magma is fixed at 20 bar, and the host rock is considered as an infinite reservoir with a constant f_{H_2} = 0.05 bar. H_2 transfer thus takes place from the magma toward the host rock. The f_{H_2} variation in the magma is computed using Equation 18 of Watson (1994), which applies to the diffusion of a volatile species in a melt in contact with a semi-infinite medium. Temperature is fixed to 800 °C and the magma is assumed to be water-saturated.

To illustrate the importance of the mobility of H_2, two values of H_2 diffusion rates were tested. The first, equal to 10^{-9} m^2/s, represents the lower limit of H_2 diffusion rate that can be inferred from our data [using $X = (D.t)^{0.5}$ with X as the capsule diameter and t, the minimum duration for observation of Fe^{3+}/Fe^{2+} change in the Ascension composition, see Table 4, no. 16]. This value is identical to that determined by Chekhmir et al. (1985) in viscous (10^{10}Pa·s) molten albite at 800 °C. Chekhmir et al. (1985) have shown that D_{H_2} is inversely correlated with viscosity (see also Watson 1994). According to their data, in a melt with a viscosity of 10^5Pa.s (corresponding to the viscosity of our experimental melts), $D_{H_2} \sim 10^{-5}$ m^2/s. We therefore adopt 10^{-5} m^2/s as an upper limit value for D_{H_2} in hydrous silicic melts at 800 °C.

Calculations were done for an imposed duration of 10 hours, which is realistic for Plinian eruptions. The results are sensitively dependent on the value taken for the H_2 diffusivity. In Figure 7A and 7B, variations of f_{H_2} and melt Fe^{3+}/Fe^{2+} are presented as a function of distance from the wall rock. Calculated

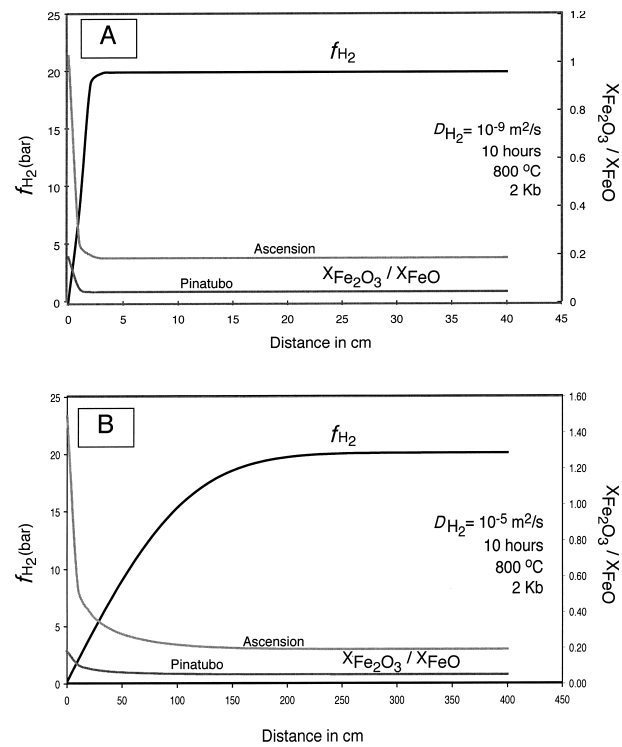

FIGURE 7. Calculation of the changes in the Fe-redox ratio ($X_{Fe_2O_3}/X_{FeO}$) of the Pinatubo and Ascension melts occurring in response to H_2 loss toward host rock. The adopted D_{H_2} is equal to 10^{-9} m^2/s.

values of melt $X_{Fe_2O_3}/X_{FeO}$ takes into account the kinetic laws identified from Equation 3 (Fig. 6) for both compositions. For log $D_{H_2} = -9$ m^2/s, a zone of ~3 cm is affected by H_2 loss and the portion of melt whose Fe^{3+}/Fe^{2+} is significantly affected remains negligible (<2 cm for both compositions, Fig. 7A). Note that the two curves nearly overlap. For log $D_{H_2} = -5$ (Fig. 7B), the f_{H_2} modifications propagate up to 2 m within the magma. For the Pinatubo composition, calculated changes in melt Fe^{3+}/Fe^{2+} propagate in the melt within the first 20 cm corresponding to a fraction of magma affected of 4% for a conduit diameter of 10 m. As a consequence, during a Plinian-type eruption of a metaluminous rhyolite with ~1 wt% FeO_T, melt $X_{Fe_2O_3}/X_{FeO}$ is not significantly affected even for the highest D_{H_2} considered because the kinetics of the $Fe^{3+} \leftrightarrow Fe^{2+}$ reaction are not fast enough in such melts. Under these conditions, glasses are therefore good indicators of pre-eruptive f_{O_2}. In contrast, similar simulations for the Ascension composition show that the melt Fe^{3+}/Fe^{2+} is significantly modified over the first 100 cm (Fig. 7B), corresponding to a fraction of magma affected of 20% for a conduit diameter of 10 m. In such a case, special care should be taken when using Fe_2O_3/FeO as indicator of pre-eruptive f_{O_2} conditions. These calculations illustrate the strong compositional control on the rate of $Fe^{3+} \leftrightarrow Fe^{2+}$ changes during ascent, and stress the need for a more precise knowledge of D_{H_2} for a correct interpretation of the Fe^{3+}/Fe^{2+} ratios of erupted lavas.

ACKNOWLEDGMENTS

This paper greatly benefited from in-depth reviews of Reid Cooper, Bjorn Mysen, and Mike Toplis. The careful editorial handling of Mike Toplis is gratefully acknowledged. This work was supported by European Community (TMR project FMRX-CT96-0063 "Hydrous Melts").

REFERENCES CITED

Baker, L. and Rutherford, MJ. (1996) The effect of dissolved water on the oxidation state of silicic melts. Geochimica Cosmochimica Acta, 60, 2179–2187.

Blank, J.G. and Brooker, R.A. (1994) Experimental studies of carbon dioxide in silicate melt: Solubility, speciation and stable carbon isotope behavior. In Ribbe, P.H., Carroll, M.R., and Holloway, J.R.,Volatiles in Magmas, 30, 157–182. Reviews in Mineralogy, Mineralogical Society of America, Washington, D.C.

Brandon, A.D. and Draper, D.S. (1996) Constraints on the origin of the oxidation state of mantle overlying subduction zones: An example from Simcoe, Washington, USA. Geochimica Cosmochimica Acta, 60, 1739–1749.

Candela, P.A. (1986) The evolution of aqueous vapor from silicate melts: effect on oxygen fugacity. Geochimica Cosmochimica Acta, 50, 1205–1211.

Carmichael, I.S.E. (1991) The redox state of basic and silicic magmas: a reflection of their source regions. Contribution to Mineralogy and Petrology, 106, 129–141.

Chekhmir, A.S., Persikov, E.S., Epel´baum, M.B., and Bukhtiyarov, P.G. (1985) Experimental investigation of the hydrogen transport through the model magmatic melt. Geokhimya, 5, 594–598.

Chou, I-M. (1986) Permeability of precious metals to hydrogen at 2Kb total pressure and elevated temperature. American Journal of Science, 286, 638–658.

Cook, G.B. and Cooper, R.F. (2000) Iron concentration and the physical processes of dynamic oxidation in alkaline earth aluminosilicate glass. American Mineralogist, 85, 397–406.

Cooper, R.F., Fanselow, J.B., and Poker, D.B. (1996) The mechanism of oxidation of a basaltic glass: Chemical diffusion of network-modifying cations. Geochimica Cosmochimica Acta, 60, 17, 3253–3265.

Devine, J.D., Gardner, J.E., Brach, H.P., Layne, G.D., and Rutherford, M.J. (1995) Comparison of microanalitical methods for estimation of H_2O content of silicic volcanic glasses. American Mineralogist, 80, 319–328.

Dingwell, D.B. and Weeb, S.L. (1990) Relaxation in silicate melts. European Journal of Mineralogy, 2, 427–449.

Gaillard, F., Scaillet, B., Pichavant, M., and Beny, J.M. (2001) The effect of water and fO_2 on the ferric-ferrous ratio of silicic melts. Chemical Geology, 174, 255–273.

Harris, C. (1983) The petrology of lavas and associated plutonic inclusions of Ascension Island. Journal of Petrology, 24, 424–470.

Hercule, S. and Ingrin, J. (1999) Hydrogen in diopside: Diffusion, kinetics of extraction-incorporation, and solubility. American Mineralogist, 84, 1577–1587.

Hess, K.-U., Dingwell, D.B., and Rössler, E. (1996) Parameterization of viscosity-temperature relations of aluminosilicate melts. Chemical Geology, 128, 155–163.

Ingrin, J. and Skogby, H. (2000) Hydrogen in nominally anhydrous upper-mantle minerals: concentration levels and implications. European Journal of Mineralogy, 12, 543–570.

Johnson, M.C., Anderson, A.T., and Rutherford, M.J. (1994) Pre-eruptive volatile contents of magmas. In Ribbe, P.H., Carroll, M.R., and Holloway, J.R., Volatiles in magmas, 30, 281–323. Reviews in Mineralogy, Mineralogical Society of America, Washington, D.C.

Kilinc, A., Carmichael, I.S.E., Rivers, M.L., and Sack, R.O. (1983) The ferric-ferrous ratio of natural silicate liquids equilibrated in air. Contribution to Mineralogy and Petrology, 83, 136–140.

Kress, V.C. and Carmichael, I.S.E. (1991) The compressibility of silicate liquids containing Fe_2O_3 and the effect of composition, temperature, oxygen fugacity and pressure on their redox states. Contribution to Mineralogy and Petrology, 108, 82–92.

Lasaga, A.C. (1998) Kinetic Theory in the Earth Sciences. Princeton series in geochemistry. 728 pp. Princeton, New Jersey.

Moore, G., Righter, K., and Carmichael, I.S.E. (1995) The effect of dissolved water on the oxidation state of iron in natural silicate liquids. Contribution to Mineralogy and Petrology, 120, 170–179.

Mysen, B.O. and Virgo, D. (1989) Redox equilibria: structure and properties of Fe-bearing aluminosilicate melts: Relationships among temperature, composition, and oxygen fugacity in the system Na_2O-Al_2O_3-SiO_2-Fe-O. American Mineralogist, 74, 58–76.

Naney, M.T. and Swanson, S.E. (1984) Iron redox kinetics in silicic melts. EOS. Transaction of American Geophysical Union, 65, 1150.

Nikolaev, G.S., Borisov, A.A., and Ariskin, A.A. (1996) New f_{O_2}–barometers for quenched glasses of various petrochemical series. Geochemistry International, 34, 9, 3–756.

Pichavant, M. (1987) Effect of B and H_2O on liquidus phase relations in the haplogranite system at 1Kbar. American Mineralogist, 72, 1056–1070.

Sack, R.O., Carmichael, I.S.E., Rivers, M., and Ghiorso, M.S. (1980) Ferric-ferrous equilibria in natural silicate liquids at 1 bar. Contribution to Mineralogy and Petrology, 75, 369–376.

Scaillet, B. and Evans, B.W. (1999) The June 15, 1991 Eruption of Mount Pinatubo. I. Phase equilibria and pre-eruption P-T-fO_2-fH_2O conditions of the dacite magma. Journal of Petrology, 40, 3, 381–411.

Scaillet, B., Pichavant, M., Roux, J., Humbert, G., and Lefèvre, A. (1992) Improvements of the Shaw membrane technique for measurement and control of fH_2 at high temperatures and pressure. American Mineralogist, 77, 647–655.

Schmidt, B.C., Scaillet, B., and Holtz, F.M. (1995) Accurate control of fH_2 in cold-seal pressure vessels with the Shaw membrane technique. European Journal of Mineralogy, 7, 893–903.

Schmidt, B.C., Holtz, F.M., and Beny, J-M. (1998) Incorporation of H_2 in vitreous silica, qualitative and quantitative determination from Raman and infrared spectroscopy. Journal of Noncrystalline solids, 240, 91–103.

Stolper, E. (1982b) The speciation of water in silicate melts. Geochimica et Cosmochimica Acta, 46, 2606–2620.

Watson, E.B. (1994) Diffusion in volatile-bearing magmas. In Ribbe, P.H., Carroll, M.R., and Holloway, J.R.,Volatiles in Magmas, 30, 371–411. Reviews in Mineralogy, Mineralogical Society of America, Washington, D.C.

Wendlandt, R.F. (1991) Oxygen diffusion in basalt and andesite melts: Experimental results and a discussion of chemical versus tracer diffusion. Contribution to Mineralogy and Petrology, 108, 463–471.

Zhang, Y., Stolper, E.M., and Wasserburg, G.J. (1991) Diffusion of water in rhyolitic glasses. Geochimica Cosmochimica Acta, 55, 441–456.

MANUSCRIPT RECEIVED JULY 10, 2001
MANUSCRIPT ACCEPTED MARCH 5, 2002
MANUSCRIPT HANDLED BY MICHAEL TOPLIS